Automatic Segmentation of Leg Bones by Using Active Contours

Sunhee Kim, Youngjun Kim, Sehyung Park, and Deukhee Lee

Abstract— **In this paper, we present a new active contours model to segment human leg bones in computed tomography images that is based on a variable-weighted combination of local and global intensity. This model can split an object surrounded by both weak and strong boundaries, and also distinguish very adjacent objects with those boundaries. The ability of this model is required for segmentation in medical images, e.g., human leg bones, which are usually composed of highly inhomogeneous objects and where the distances among organs are very close. We developed an evolution equation of a level set function whose zero level set represents a contour. An initial contour is automatically obtained by applying a histogram based multi-phase segmentation method. We experimented with computed tomography images from three patients, and demonstrate the efficiency of the proposed method in experimental results.**

I. INTRODUCTION

Image segmentation is to decompose an image into several regions with similar properties, such as shape, color, or intensity, etc. In this work, we are interested in the intensity based segmentation. It is a fundamental task for image processing and computer vision, and required in various applications, such as medical, biological, and industrial fields. Images from real applications, e.g., human leg bones in medical images, are usually highly inhomogeneous, which means the distribution of intensity in each object is not regular. It causes one object to have both weak and strong boundaries irregularly, which generates dappled boundaries. And the distance among objects with dappled boundary is very close that necessitates a delicate segmentation model. Many successful segmentation models [1]-[5] for inhomogeneous images have been developed. They all use local approximations of intensity inside and outside the contour so that they can deal with image inhomogeneity. But they do not work for images containing an object with dappled boundaries, and also cannot distinguish the adjacent objects with dappled boundaries, which is not appropriate for segmentation of leg bones in computed tomography(CT) images. An elaborate segmentation of leg bone is needed for an accurate surgical planning in anterior cruciate ligament reconstruction. To overcome the limitation of previous methods, we propose a new active contours model that uses a variable-weighted combination of both local and global approximations of intensity inside and outside the contour. And we apply a histogram based multi-phase segmentation method [6] to the given three-dimensional data in order to automatically obtain an initial contour for the proposed segmentation method. Through experimental results, we will demonstrate the efficiency of the proposed method for automatic segmentation of leg bones in CT images.

This work was supported by the Korea Institute of Technology Institutional Program under Grant No.2E24520 and No.2E25116.

S. Kim, Y. Kim, S. Park, and D. Lee are with the Center for Bionics, Korea Institute of Science and Technology, Seoul, Korea skim2227@gmail.com, junekim@kist.re.kr, sehyung@kist.re.kr, and dkylee@kist.re.kr

II. METHOD

Let $f : \Omega \times \{1, \cdots, m\} \subset \mathbb{R}^2 \times \mathbb{N} \to \mathbb{R}$ be a given CT data, where m is the number of sliced images in a volume data. Before segmentation procedure, we first adjust the data intensity in order to suppress intensities of background regions outside bones; $f(x,y,z) = 0$ if $f(x,y,z) < 0$, and the effect can be observed in Fig. 1. In CT images, the hounsfield unit(HU) of bones range from 80 to 200, and very weak bones have the values close to 80HU. In order to distinguish the background and those bones, we use the value of 0 not 80 in image adjustment. The left image is original and the right image is the result of adjustment.

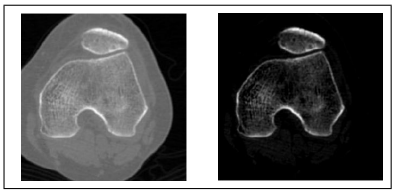

Fig. 1. Example of adjustment of image intensity.

A. Histogram Based Multi-phase Segmentation Method

Given a data f, we can construct its histogram $g : D = [min(f), max(f)] \to \mathbb{R}$ by counting the number of pixels contained in each bin. In [6], Kim et al. proposed a method to find the number of different regions automatically by using one-dimensional histogram, and performed a region-based segmentation on the given data with information obtained from the histogram. They observed that the number of meaningful local maxima in a histogram reflects the number of different regions on an image. The goal is to decompose a domain D of an initial histogram into several subdomains of D and the remaining set Q. Each subdomain D_i contains the global maximum of the i-th histogram that is obtained by removing from the first to $(i-1)$-th histogram from the original histogram. The necessary information of the removed histogram was extracted through the previous steps. The set Q is the domain of the $(n+1)$-th histogram such that $max_{s \in Q} g(s)$ is very small compared to the original histogram, or Q is empty. This is a redundant set in searching a meaningful local maxima because such regions associated with very small histogram values are usually useless in image segmentation. Then, the number of different regions is n.

978-1-4244-7929-0/14/$26.00 ©2014 IEEE

To find each subdomain D_i containing the global maximum of the i-th histogram, they repetitively conduct the standard 2-means clustering under some rules below. For an image histogram, the 2-means clustering problem is described as

$$argmin_{R_1,R_2} \sum_{j=1}^{2} \sum_{s\in R_j} g(s)(s-r_j)^2,$$

where each center r_j is computed by $r_j = \frac{\sum_{s\in R_j} s\, g(s)}{\sum_{s\in R_j} g(s)}$ for $j = 1,2$. And the suggested rules are as follows:

- **Rule 1.** choose a cluster

$$R^* = \begin{cases} R_1 & \text{if } max_{s\in R_1} g(s) > max_{s\in R_2} g(s) \\ R_2 & \text{otherwise} \end{cases}$$

- **Rule 2.** $|argmax_{s\in R_1} g(s) - argmax_{s\in R_2} g(s)| < \omega_1$
- **Rule 3.** $max_{s\in D-\cup_{j=1}^{i-1} D_j} g(s) < \omega_2\, mean_D(g)$

The first rule explains that we select the cluster containing the larger maximum histogram value between two clusters, R_1 and R_2; and we apply the 2-means clustering only to the selected cluster again. We repeat this procedure until the second rule is satisfied, and then we get the i-th subdomain D_i of D. The parameter ω_1 represents the least difference in intensities of distinct regions, which assures that the regions with similar intensities are not split according to ω_1. In our experiment, we used $\omega_1 = 10$ or 20. In the last rule, $mean_D(g)$ is the average value of the original histogram, and $max_{s\in D-\cup_{j=1}^{i-1} D_j} g(s)$ is the maximum value of the i-th histogram which is the reduced histogram after finding $i-1$ subdomains D_i. The parameter ω_2 prevents from finding too small local maxima compared to the original histogram, which denotes usually unnecessary region to be segmented. We used $\omega_2 = 0.1$ in this application. If the last rule is satisfied, the process with histogram is accomplished. From this procedure, we automatically get the number, n, of distinct regions and the n subdomains $\{D_i\}_{i=1}^n$.

After then, the region-based segmentation by level set function is performed to allocate the regions corresponding to Q and compensate the coherence of regions. In each subdomain D_i, a center d_i is computed by $d_i = \frac{\sum_{s\in D_i} s\, g(s)}{\sum_{s\in D_i} g(s)}$, and an initial level set function is defined as a labeling function;

$$\phi(x,y,z) = \begin{cases} 1 & \text{if } f(x,y,z) \le \frac{d_1+d_2}{2} \\ i & \text{if } \frac{d_{i-1}+d_i}{2} < f(x,y,z) \le \frac{d_i+d_{i+1}}{2} \\ n & \text{if } \frac{d_{n-1}+d_n}{2} < f(x,y,z) \end{cases} \quad (1)$$

for $2 \le i \le n-1$. The authors suggested a fast and simplified segmentation algorithm as follows: in each region $\{(x,y,z) : \phi(x,y,z) = i\} \subset \Omega \times \{1,\cdots,m\}$ for $2 \le i \le n$,

$$\text{update } \phi(x,y,z) = i-1 \text{ when } \frac{c_{i-1}+c_i}{2} < f(x,y,z),$$

where

$$c_i(\phi) = \frac{\int_1^m \int_\Omega f\,\{H(\phi-i) - H(\phi-(i+1))\}}{\int_1^m \int_\Omega \{H(\phi-i) - H(\phi-(i+1))\}}.$$

Here, the function $H(\eta)$ equals 1 if $\eta \ge 0$ and equals 0 if $\eta < 0$. Clearly, the constant c_i is the average value of intensities f in each region $\{(x,y,z) : \phi(x,y,z) = i\}$.

B. Proposed Method

From the histogram based multi-phase segmentation method, we have n-labelled data. According to the property of desirable objects, the region of interest can be chosen differently by setting the different number of label. In our experiments, we set the label l_0=2. We define an initial function u for an elaborate segmentation as follows:

$$u(x,y,z) = \begin{cases} +1 & \text{if } \phi(x,y,z) \ge l_0 \\ -1 & \text{otherwise.} \end{cases}$$

For the unity of parameters in all sliced images of one volume data, we fill the hole of each initial function in the two-dimension. Then we make the initial contour $\{(x,y,z) : u(x,y,z) = 0\}$ surround the desirable objects by blurring the filled initial function, and binarizing it into +1 and -1, also denoted by u. Fig. 2 shows the results of the histogram based multi-phase segmentation method and their corresponding initial functions. The first column is the adjusted data on intensity, and the second column is the result of the multi-phase segmentation method for the first column data. And the yellow contours in the last column indicate the initial contours, i.e., $\{(x,y,z) : u(x,y,z) = 0)\}$ automatically obtained. These initial contours are the good initializations for all slices which lead fast convergence as well as the correct segmentation.

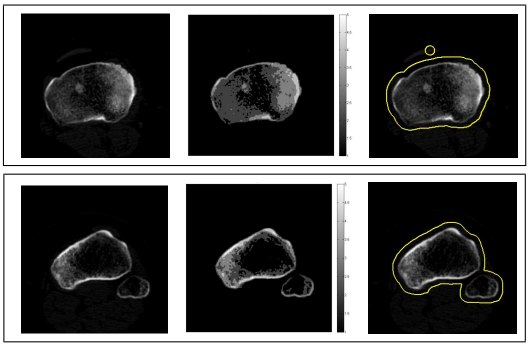

Fig. 2. Histogram based multi-phase segmentation method and automatically obtained initial functions

So far, we have a given three-dimensional CT data $f(x,y,z) : \Omega \times \{1,\cdots,m\} \to \mathbb{R}$ and an initial level set function $u(x,y,z) : \Omega \times \{1,\cdots,m\} \to [-1,+1]$ derived from the histogram based multi-phase segmentation. A new method for delicate segmentation is developed for each sliced image by fixing $z_0 \in \{1,\cdots,m\}$, and we denote $f(x,y) : \Omega \times \{z_0\} \to \mathbb{R}$ and $u(x,y) : \Omega \times \{z_0\} \to [-1,1]$. We introduce two forces, global and local forces, by following the idea of Zhang et

al.[3], and then suggest a variable-weighted combination of the two forces. First, a global force is defined as

$$F_g(x,y) = f(x,y) - \frac{\alpha_1 c_1 + \alpha_2 c_2}{\alpha_1 + \alpha_2}, \tag{2}$$

where two parameters α_1 and α_2 are positive such that $\alpha_1 + \alpha_2 = 2$. Here, c_1 is the average value of f in $\{(x,y) : u(x,y) > 0\}$ and c_2 is the average value of f in $\{(x,y) : u(x,y) < 0\}$. Since c_1 and c_2 are global averages, the force F_g has itself a global property. An evolution with the global force is very fast and easy, but cannot segment correctly an image with both strong and weak boundaries, because it depends only on the global average values.

Local information, such as the distribution of intensities in a small neighborhood, is necessary in order to deal with weak boundaries. The local force F_l is defined similarly to the global force F_g as

$$F_l(x,y) = f(x,y) - \frac{\beta_1 s_1(x,y) + \beta_2 s_2(x,y)}{\beta_1 + \beta_2}, \tag{3}$$

where two parameters β_1 and β_2 are positive such that $\beta_1 + \beta_2 = 2$. The functions $s_1(x,y) = \frac{G_{\sigma_l} * [H(u) \otimes f]}{G_{\sigma_l} * H(u)}$ and $s_2(x,y) = \frac{G_{\sigma_l} * [(1-H(u)) \otimes f]}{G_{\sigma_l} * (1-H(u))}$ are smooth approximations of f inside and outside the zero level set of u. The notations $*$ and $\otimes$ denote the convolution operator and the element-wise product, respectively. Here, G_{σ_l} is a Gaussian kernel with standard deviation σ_l which determines the locality. Since two functions s_1 and s_2 are local average values, F_l has a local property. The different values of β_1 and β_2 affect location details of the contour. By solving an evolution equation with the local force F_l, we can find local details. However, since the strength of the local force is very low in the smooth region, the final contour may be stuck in wrong locations or retain undesirable fractions over the smooth region, which degrades the evolution rate and segmentation quality.

We have found that evolution with the global force is very fast, but fails to extract local details, while local force based evolution captures stained boundaries successfully, but with very slow computation and undesirable fractions. Hence, we suggest a new force F that integrates the advantages of F_g and F_l. We observed that in practice, each pixel requires different weights for each force, which means that some pixels need to put more weight on the global force, while others require more weight on the local force.

As an indicator of different weights, we introduce a variable weight function $W : \Omega \subset \mathbb{R}^2 \to \mathbb{R}$

$$W(x,y) = |f(x,y) - mean(N_h^f(x,y))|, \tag{4}$$

where $N_h^f(x,y) = \{f(\tilde{x},\tilde{y}) : (\tilde{x},\tilde{y}) \in [x-h, x+h] \times [y-h, y+h]\}$ for a positive integer h. This represents the local difference in intensity between f and the local average $mean(N_h^f(x,y))$. A high value of $W(x,y)$ indicates the local edge where the intensities change rapidly in a neighborhood centered at (x,y). The ability to find a local edge is required to capture a dappled boundary successfully. A low value of $W(x,y)$ signifies the local smoothness that the intensities vary smoothly in a neighborhood. We note that a two-dimensional neighborhood is used in the computation of W. If a three dimensional neighborhood is used, strong edges in the upper or lower slices might interrupt the capture of weak edge in the present slice.

Two objectives in constructing the new force F are as follows. (i) In a region where the values of W are low, we use the global force. (ii) In a region where the values of W are high, we use the local force. If W is low, the local variance of intensity is small, so it does not need to be observed locally. Thus, we can use the global force in a locally smooth region. On the other hand, if W is high, the local variance of intensity is large. This necessitates the use of the local force to observe the local details not captured by the global force. From the objectives, we define a local-global force F with a variable weight W as

$$F(x,y) = \frac{\alpha(1-W(x,y))F_g(x,y) + \beta W(x,y) F_l(x,y)}{\alpha + \beta}.$$

The local force in the region where W is large enables the capture of weak boundaries, and the global force in the region where W is small prevents undesirable fractions in the segmentation. The variable weight function W indicates which force should be used with more weight for each pixel. Using the variable weight W enables us to extract necessary information and suppress unnecessary information relating to F_l and F_g.

We also observe that even if one of the parameters α or β vanishes, the other force does not affect all of the pixels as much as original values of that force would. For example, even if F is dominated by F_l by setting $\alpha = 0$, F_l will have less impact on the region where the value of W is low, but will have more impact on the region where the value of W is high. Thus, even though the local force F_l is used in the smooth region, the low value of W discounts unnecessary information about F_l, the cause of undesirable fractions in smooth regions.

Ideally, W takes the value one on local edges and zero in locally smooth regions. But, in practice, W has relative values in the neighborhood of each pixel, so the difference in W between local edges and locally smooth regions may be much smaller than one. In this case, the two auxiliary parameters α and β are chosen as different values to accentuate the difference, for example, $\alpha = 0.1$ and $\beta = 1.9$.

We construct the final evolution equation by adding smoothing term Δu of u and restricting the evolution region to the neighborhood of contours with $|\nabla u|$:

$$\begin{aligned} &\frac{\partial u}{\partial t}(x,y) = (F(x,y) + \mu \Delta u(x,y))|\nabla u(x,y)|, \\ &F(x,y) = \frac{\alpha(1-W(x,y))F_g(x,y) + \beta W(x,y) F_l(x,y)}{\alpha + \beta}. \end{aligned} \tag{5}$$

The algorithm is as follows.

Require given data f, initial u, and parameters
for $z = 1, \cdots, m$
Compute a variable-weight function W using (4)
repeat
(i) Compute a global force F_g using (2)
(ii) Compute a local force F_l using (3)
(iii) Compute a total force F and update u using (5)
(iv) Implement $u = (u > 0) - (u < 0)$ and $u = u * G_\sigma$, where G_σ is a Gaussian kernel with a standard deviation σ to regularize u
until $|u^{new} - u^{old}| < \varepsilon$
end

III. Experimental Results

We experimented with CT data from three patient and our programming environment for all experiments is Matlab 8.0 on a 3.5 GHz Intel i7 personal computer. The original image was clipped to save the computational time but containing all two-dimensional bones, and those sizes are indicated in the second column of Table 1. Common parameters of the proposed method for all data is as follows: $dt = 300$, $\sigma_l = 5$, $h = 10$, and $\alpha = 0.05$. If α, α_1, and β_1 are chosen, the corresponding values β, α_2, and β_2 are automatically determined by: $\beta = 2 - \alpha$, $\alpha_2 = 2 - \alpha_1$, and $\beta_2 = 2 - \beta_1$. The different parameters are shown in Table 1 and we also present the computational cost in CPU time for each data. The value $t1$ is a time for the histogram-based segmentation method, and the value $t2$ is for the new segmentation method.

TABLE I

data	size	μ	σ	α_1	β_1	t1	t2
1	256×297×293	0.01	1.5	0.9	1.2	56.3s	1104.5s
2	328×324×421	0.01	1.2	1	0.8	97.9s	1803.2s
3	319×385×351	0.02	1.5	0.9	1.2	38.5s	1971.4s

We illustrated some elaborate segmentations of the proposed method in Fig. 3. The first column shows the images to be segmented, and the second column is the segmentation results. In the last column, we plotted the zoom of regions in the green boxes of the first and second columns, which demonstrates the efficiency of the new method. And we also reconstructed the surface from the segmented data, as displayed in Fig. 4. The proposed model can perform a correct segmentation of objects with both strong and weak boundaries as well as split the adjacent objects in detail. We will implement with more database, and prove the robustness of parameters and accuracy of segmentation in future work.

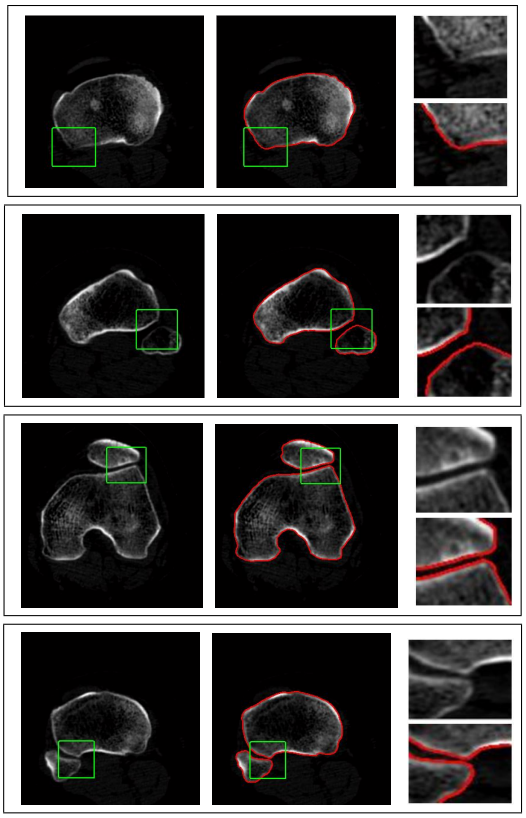

Fig. 3. Elaborate segmentation of the proposed method.

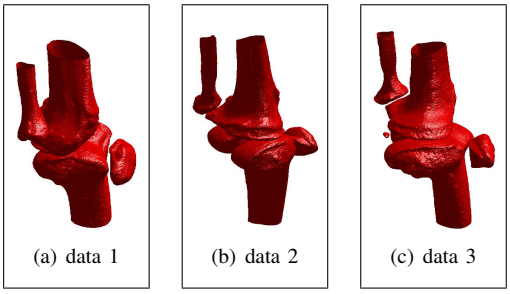

(a) data 1 (b) data 2 (c) data 3

Fig. 4. Surface Reconstructions.

References

[1] C. Li, C.Kao, Z. Ding, Implicit active contours driven by local binary fitting energy, in Proceedings of the IEEE Conference on Computer Vision and Pattern Recognition(CVPR), 2007, pp. 1-7.

[2] C. iL, C.Kao, J.C. Gore, Z. Ding, Minimization of region-scalable fitting energy for image segmentation, IEEE Transactions on Image Processing 17(10), 2009, pp. 1940-1949.

[3] K. Zhang, L. Zhang, H. Song, W. Zhou, Active contours with selective local or global segmentation: a new formulation and level set method, Image and Vision Compution, 28(4), 2010, pp. 668-676.

[4] T. Tran, V. Pham, Y. Chiu, K. Shyu, Active contour with selective local or global segmentation for intensity inhomogeneous image, in Proceedings of the 3rd IEEE International Conference on Computer Science and Information Technology, 2010, pp.306-310.

[5] S. Liu, Y. Peng, A Local Region-based Chan-Vese Model for Image SEgmentation, Pattern Recognition, 45, 2012, pp.2769-2779.

[6] S. Kim and M. Kang, Multiple-region segmentation without supervision by adaptive global maximum clustering, IEEE Transactions on Image Processing, 21(4), 2012, pp.1600 -1612.

[7] T. Chan, L.A. Vese, Active contours without edges, IEEE Transactions on Image Processing 10, 2001, pp. 266-277.

[8] S. Osher, J.A. Sethian, Fronts propagating with curvature dependent speed: algorithms based on Hamilton-Jacobi formulations, Journal of Computational Physics, 79, 1988, pp. 12-49.

[9] H. Zhou, X. Li, G. Schaefer, M. Emre Celebi, P. Miller, Mean shift based gradient vector flow for image segmentation, Computer Vision and Image Understanding, 117(9), 2013, pp. 1004-1016.

[10] H. Zhou, G. Schaefer, T. Liu, F. Lin, Segmentation of optic disc in retinal images using an improved gradient vector flow algorithm, Multimedia Tools Applications, 49(3), 2010, pp. 447-462.